Dynamical structure factors for dimerized spin systems

2003 J. Phys.: Condens. Matter 15 8513

(http://iopscience.iop.org/0953-8984/15/49/025)

INSTITUTE OF PHYSICS PUBLISHING JOURNAL OF PHYSICS: CONDENSED MATTER

J. Phys.: Condens. Matter **15** (2003) 8513–8526 PII: S0953-8984(03)64846-0

Dynamical structure factors for dimerized spin systems

M Müller[1], H-J Mikeska[1] and N Cavadini[2]

[1] Institut für Theoretische Physik, Universität Hannover, Appelstrasse 2, D-30167 Hannover, Germany
[2] Laboratory for Neutron Scattering, ETH Zürich and Paul Scherrer Institut, CH-5232 Villigen PSI, Switzerland

Received 10 June 2003, in final form 16 September 2003
Published 25 November 2003
Online at stacks.iop.org/JPhysCM/15/8513

Abstract

We discuss the transition strength between the disordered ground state and the basic low-lying triplet excitation for interacting dimer materials by presenting theoretical calculations and series expansions as well as inelastic neutron scattering results for the material $KCuCl_3$. We describe in detail the features resulting from the presence of two differently oriented dimers per unit cell and show how energies and spectral weights of the resulting two modes are related to each other. We present results from the perturbation expansion in the interdimer interaction strength and thus demonstrate that the wavevector dependence of the simple dimer approximation is modified in higher orders. Explicit results are given in tenth order for dimers coupled in 1D, and in second order for dimers coupled in 3D with application to $KCuCl_3$ and $TlCuCl_3$.

1. Introduction

Low-dimensional quantum antiferromagnets have received much interest in recent years since they serve as model substances allowing us to investigate in detail the effects of quantum fluctuations and to test theoretical models. One important class of materials in this context consists of an assembly of dimers (two strongly coupled spins $1/2$) which interact sufficiently weakly to guarantee that the dimer gap does not close. These materials are characterized by a disordered singlet ground state and a finite spin gap to triplet excited states. Prominent examples in this class are $KCuCl_3$ and $TlCuCl_3$ which have been investigated in detail in the last years by static and dynamic methods as well as theoretically [1]. The most detailed experimental information is obtained from inelastic neutron scattering (INS) experiments, which directly explore the basic singlet–triplet transition in all of reciprocal space [2, 3].

The energy of the singlet–triplet transition along the principal axis in reciprocal space as measured in these experiments is well described by the model of interacting dimers; to lowest order this is formulated as the effective dimer model [4, 5], and it has been refined by

0953-8984/03/498513+14$30.00

perturbative cluster expansions up to sixth order [3]. Here we supplement this analysis by discussing the dynamical structure factor.

The dynamical structure factor for spins localized on a Bravais lattice is defined as

$$S^{\alpha\beta}(\mathbf{q},\omega) = \int_{-\infty}^{\infty} \mathrm{d}t\ \mathrm{e}^{-\mathrm{i}\omega t}\langle \mathcal{S}^{\alpha}(\mathbf{q},t)\mathcal{S}^{\beta}(-\mathbf{q},0)\rangle \tag{1}$$

where

$$\mathcal{S}^{\alpha}(\mathbf{q},t) = \sum_{\mathbf{R}} \mathrm{e}^{-\mathrm{i}\mathbf{q}\mathbf{R}}\mathcal{S}^{\alpha}(\mathbf{R},t) \tag{2}$$

is the Fourier transformation of the spin operators at lattice sites $\mathbf{R}$. The superscripts α, β denote the spin components and the brackets $\langle\cdots\rangle$ thermal expectation values (which for $T = 0$ reduce to ground-state expectation values $\langle 0|\cdots|0\rangle$). Apart from known prefactors, equation (1) reflects the spectral weight from the magnetic neutron scattering cross section [6].

If we consider transitions from the ground state $|0\rangle$ to some well defined eigenstate $|n\rangle$ with energy $\omega_n(\mathbf{q})$, we obtain δ-peaked contributions to the dynamical structure factor

$$S^{\alpha\beta}(\mathbf{q},\omega) = \sum_{n}\langle 0|\mathcal{S}^{\alpha}(\mathbf{q})|n\rangle\langle n|\mathcal{S}^{\beta}(-\mathbf{q})|0\rangle\delta(\omega-\omega_n(\mathbf{q})) \tag{3}$$

$$= \sum_{n} I_n^{\alpha\beta}(\mathbf{q})\delta(\omega-\omega_n(\mathbf{q})). \tag{4}$$

In interacting dimer materials, INS probes directly the transition from the (singlet) ground state $|0\rangle$ to the lowest (triplet) excitation $|\mathrm{t}\rangle$ and we will reduce our discussion to this contribution to the dynamical structure factor. Owing to the rotational symmetry of the underlying Heisenberg model it is sufficient to calculate $I_{\mathrm{t}}^{zz}(\mathbf{q})$ only and we use the shorthand $I_{\mathrm{sm}}(\mathbf{q}) := I_{\mathrm{t}}^{zz}(\mathbf{q})$ to denote the lowest triplet (single magnon) contribution to the spectral weight.

The INS investigation of the materials $KCuCl_3$ and $TlCuCl_3$ at finite magnetic fields provides direct verification of this point as reported in [7].

The discussion of our results is organized as follows. In section 2 we will give theoretical results for a 1D array of interacting dimers. This model has been treated before [8]; it is, however, instructive to demonstrate for the simple 1D case that existing standard expansions are modified by additional terms which emerge starting in second order. In addition we present the quantitative changes for the transition strength comparing first order to tenth order results to show the effect of high order calculations. In section 3 we discuss interacting dimers in a 3D network by presenting in parallel neutron scattering results for the material $KCuCl_3$ and series expansions to second order. The same type of additional term as in 1D is obtained in this calculation and corrects the results for the dynamical structure factor as obtained in the random phase approximation (RPA) before; see [9]. These RPA results are found to be correct only to first order. Section 4 gives our conclusions.

2. Alternating chain

First we consider the one-dimensional (1D) alternating $S = 1/2$ spin chain with isotropic nearest-neigbour interactions. The Hamiltonian of this model is of the following form:

$$\mathcal{H} = J\sum_{n=1}^{N}(\mathbf{S}_1(n)\cdot\mathbf{S}_2(n) + \lambda\mathbf{S}_2(n)\cdot\mathbf{S}_1(n+1)), \qquad J > 0. \tag{5}$$

Here, the alternating chain is described as a system with N unit cells with two spins each and periodic boundary conditions are used. There are two exchange constants, J and λJ; for $\lambda = 0$ the ground state of the system consists of singlets on the intracell bonds $(n,1)-(n,2)$. These

local singlets can be excited to triplets which remain gapped excitations when switching on λ, $0 < \lambda < 1$. In the limit $\lambda = 1$ we arrive at the well known Heisenberg antiferromagnet (HAFM) with pairs of $S = 1/2$ spinons as lowest gapless excitations. Other related models are described in [10].

The triplet excitation energies $\omega(q)$ have been obtained by perturbation expansion in λ up to ninth order in [8] and to tenth order in [5] using the cluster expansion approach.

2.1. The dynamical structure factor

Turning to the calculation of the structure factor for a system with Hamiltonian (5), we note (see equations (1) and (2)) that for this calculation we have to specify the positions of the spins, **R**, in space (whereas the eigenvalues depend solely on the exchange constants). In a slight generalization of a strictly linear geometry we allow for our calculation the separation **d** of two spins in one unit cell to be different in magnitude and direction from the separation **a** of two adjacent spins in different unit cells (note that **a** defines the overall chain direction). The resulting geometry is shown in figure A.1 and makes clear the relation to the real 3D systems to be dealt with in the next section: the 1D chain defined in equation (5) can alternatively be looked at as a ladder with rung and diagonal interactions only. For the chain geometry shown in figure A.1 the spectral intensity up to first order in λ is obtained as follows:

$$I_{\mathrm{sm}}(\mathbf{q}) = \sin^2 \frac{\mathbf{qd}}{2}\left(1 + \frac{1}{2}\lambda\cos(\mathbf{qa})\right) + \mathcal{O}(\lambda^2). \tag{6}$$

Here, **q** is the wavevector, **d** and **a** the separation of the spin sites within and between the dimers, respectively. We note that the term $\propto \sin^2(\mathbf{qd}/2)$ is typical for systems consisting of isolated dimmers; it is known as the dimer structure factor [11]. The first order correction in λ adds an additional modulation to the intensity, which depends on the ratio $\sigma = \|\mathbf{d}\|/\|\mathbf{a}\|$.

Using the cluster expansion method (see appendix A) we have systematically calculated the series in λ for the intensity up to the tenth order. This requires linked clusters consisting of a maximum of ten bonds. The resulting series can be split into three different terms:

$$I_{\mathrm{sm}}(\mathbf{q}) = B_{\mathrm{c}}(\mathbf{q}, \lambda) + B_{\mathrm{s}}(\mathbf{q}, \lambda) + \Lambda(\mathbf{q}, \lambda). \tag{7}$$

To illustrate the result we give the series up to fourth order[3]:

$$\begin{aligned} B_{\mathrm{c}}(\mathbf{q}, \lambda) &= \sin^2 \frac{\mathbf{qd}}{2} \sum_{j=0}^{4} \mu_j \cos(j\mathbf{qa}), \\ B_{\mathrm{s}}(\mathbf{q}, \lambda) &= \sin \mathbf{qd} \sum_{j=0}^{4} \nu_j \sin(j\mathbf{qa}) \end{aligned} \tag{8}$$

where

$$\begin{aligned} \mu_0 &= 1 - \tfrac{5}{16}\lambda^2 - \tfrac{3}{32}\lambda^3 + \tfrac{25}{1536}\lambda^4, & \nu_0 &= 0, \\ \mu_1 &= \tfrac{1}{2}\lambda - \tfrac{1}{8}\lambda^2 - \tfrac{5}{192}\lambda^3 + \tfrac{41}{2304}\lambda^4, & \nu_1 &= \tfrac{1}{8}\lambda^2 + \tfrac{7}{192}\lambda^3 - \tfrac{131}{4608}\lambda^4, \\ \mu_2 &= \tfrac{3}{16}\lambda^2 + \tfrac{7}{48}\lambda^3 + \tfrac{23}{1024}\lambda^4, & \nu_2 &= \tfrac{1}{96}\lambda^3 + \tfrac{25}{4608}\lambda^4, \\ \mu_3 &= \tfrac{5}{64}\lambda^3 + \tfrac{155}{2304}\lambda^4, & \nu_3 &= \tfrac{23}{2304}\lambda^4, \\ \mu_4 &= \tfrac{35}{1024}\lambda^4, & \nu_4 &= 0, \end{aligned} \tag{9}$$

and

$$\Lambda(\mathbf{q}, \lambda) = \tfrac{1}{128}\lambda^4(\cos(2\mathbf{qd}) - \cos(2\mathbf{qa})). \tag{10}$$

[3] Higher order terms are available on request.

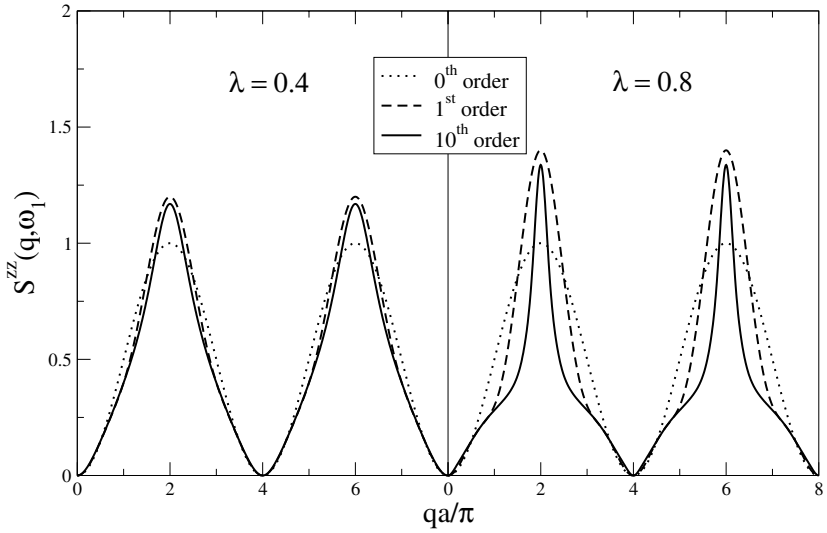

Figure 1. Structure factor with $\lambda = 0.4, 0.8$, $\mathbf{a} \parallel \mathbf{d}$ and ratio $d/a = 10/20$.

The terms in $B_c(\mathbf{q}, \lambda)$ are consistent with previous publications [8], whereas $B_s(\mathbf{q}, \lambda)$ and $\Lambda(\mathbf{q}, \lambda)$ contain additional corrections. They originate from a complete expansion of both the ground state $|0\rangle$ and the first excited state $|t\rangle$. If one assumes that $\langle 0|S_{2i}|t\rangle = -\langle 0|S_{2i+1}|t\rangle$ for the matrix elements on even and odd sites, one ends up with $B_c(\mathbf{q}, \lambda)$ only. However this is only correct to first order and in general we have $\langle 0|S_{2i}|t\rangle \neq -\langle 0|S_{2i+1}|t\rangle$. This inequality arises from virtual states with odd parity under exchange of two triplets which occur during the perturbation expansion for the first time in second order.

In figures 1 and 2 we show some typical plots of the intensity $I_{sm}(\mathbf{q})$ for two different ratios $\sigma = 10/15$ and 10/20, two different coupling strengths $\lambda = 0.4$ and 0.8 and strictly linear geometry, $\mathbf{d} \parallel \mathbf{a}$ (then, only the component of the wavevector in the chain direction enters). The difference between the zeroth and the first order emerge very clearly. The higher order terms emphasize the modulation originating from the two length scales $\|\mathbf{a}\|$ and $\|\mathbf{d}\|$.

2.2. Sum rule

The total integrated scattering intensity has a well defined magnitude, determined by the local spin length through the following sum rule:

$$\mathcal{I} = \sum_{\alpha} \frac{\int \mathrm{d}\mathbf{q} \int (\mathrm{d}\omega/2\pi) S^{\alpha\alpha}(\mathbf{q}, \omega)}{\int \mathrm{d}\mathbf{q}} = S(S+1). \tag{11}$$

For the one-dimensional alternating chain the contribution from the one-magnon part to the total spectral weight is calculated from equation (7); the integral reduces to the constant part μ_0 of (9), since only non-oscillating terms survive the integration:

$$\mathcal{I}_{sm} = \tfrac{3}{4}(1 - \tfrac{5}{16}\lambda^2 - \tfrac{3}{32}\lambda^3 + \tfrac{25}{1536}\lambda^4 + \cdots) \leqslant \tfrac{3}{4} \qquad S = \tfrac{1}{2}, \quad \lambda \ll 1. \tag{12}$$

For the non-interacting case ($\lambda = 0$) the sum rule is exhausted by the one-triplet excitation since it is an exact eigenstate: From (3) we see that this excitation gives the only non-vanishing matrix element. Switching on the coupling between the dimers, more and more intensity goes in two- or more-magnon scattering processes. A theoretical discussion of the multimagnon states for the one-dimensional alternating chain is given in [8, 12, 13].

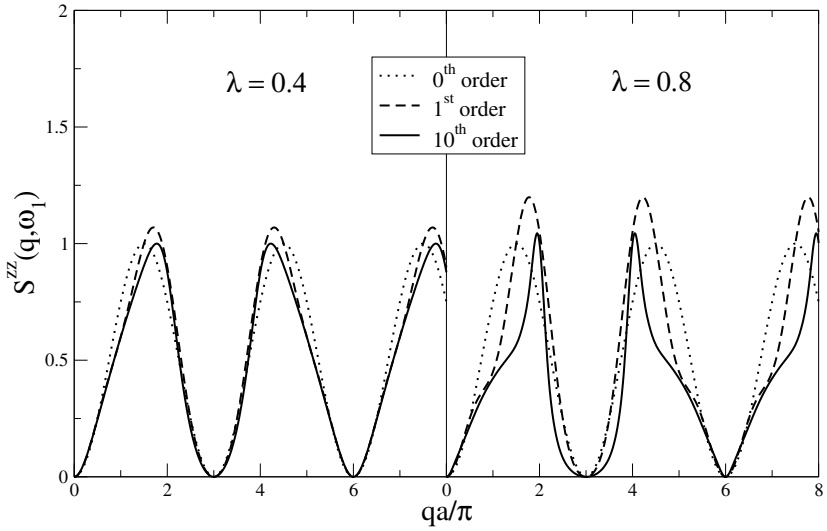

Figure 2. Structure factor with $\lambda = 0.4, 0.8$, $\mathbf{a} \parallel \mathbf{d}$ and ratio $d/a = 10/15$.

3. The 3D dimer substances $KCuCl_3$ and $TlCuCl_3$

In this section we extend the calculation of singlet–triplet intensities to three-dimensional substances such as $KCuCl_3$ and $TlCuCl_3$. These compounds are weakly interacting quantum spin systems which exhibit an excitation gap. Similar to the alternating chain discussed in the previous section, this is based on the existence of strongly interacting bonds forming dimers. In these materials the orientation of the dimers alternates, i.e. each unit cell consists of four spins with two differently oriented dimers.

The following considerations are valid for dimer systems composed of two dimers per unit cell. We write for the Fourier transformed spin operators

$$S^z(\mathbf{q}) = \frac{1}{\sqrt{2N}} \sum_{\mathbf{n}} \sum_{k=1}^{2} \mathrm{e}^{-\mathrm{i}\mathbf{q}(\mathbf{n}+\mathbf{R}_k)} \left[\mathrm{e}^{-\mathrm{i}\frac{\mathbf{q}\mathbf{d}_k}{2}} S^z\left(\mathbf{n} + \mathbf{R}_k + \frac{\mathbf{d}_k}{2}\right) + \mathrm{e}^{\mathrm{i}\frac{\mathbf{q}\mathbf{d}_k}{2}} S^z\left(\mathbf{n} + \mathbf{R}_k - \frac{\mathbf{d}_k}{2}\right) \right], \quad (13)$$

where $\mathbf{n}$ denotes the unit cell, $\mathbf{R}_k$ the centre of the dimer and $\mathbf{d}_k$ the separation of the two spins forming the dimer. The first sum in (13) is taken over all unit cells. In the case of weakly interacting dimers the localized triplet states are replaced by Bloch-like triplet modes which propagate due to the interaction network between the dimer units. The details of the explicit calculation of the transition matrix elements for a Bravais dimer lattice are illustrated in [8].

In table 1 we describe the interaction network listing the basic lattice vectors associated with non-zero interdimer interactions for the materials considered. In table 2 we give the numerical values of the intradimer exchange J (in meV) and of the interdimer exchange interactions (in relative units) for the compounds $KCuCl_3$ and $TlCuCl_3$. (Slightly improved values for $KCuCl_3$ have been determined in [17]; the difference, however, is not visible in figures 3 and 5.)

The different dimer orientations in the unit cell do not affect the dimer lattice directly, i.e. the lowest excitation does not depend on the dimer orientation. But the full translational symmetry is obviously reduced if the dimer sites are distinct by their orientation.

In analogy to phonons in a lattice with a basis there will be two excitation modes. Therefore we use the following zeroth order ansatz for the one-triplet wavefunction, which manifests

Table 1. Considered interactions in $KCuCl_3$ (and $TlCuCl_3$). Vectors $\mathbf{g}_k$ denote the distances between the dimer centres.

Distance $\mathbf{g}_k$ between dimers	Interactions between	
	Equivalent spins ($i = j$)	Non-equivalent spins ($i \neq j$)
$\mathbf{g}_1 = \mathbf{a}$	$J_{(100)}$	$J'_{(100)}$
$\mathbf{g}_2 = 2\mathbf{a} + \mathbf{c}$	—	$J'_{(201)}$
$\mathbf{g}_3 = \mathbf{a} + \frac{1}{2}(\mathbf{b} + \mathbf{c})$	$J_{(1\frac{1}{2}\frac{1}{2})}$	$J'_{(1\frac{1}{2}\frac{1}{2})}$
$\mathbf{g}_4 = \mathbf{a} - \frac{1}{2}(\mathbf{b} - \mathbf{c})$	$J_{(1\frac{1}{2}\frac{1}{2})}$	$J'_{(1\frac{1}{2}\frac{1}{2})}$

Table 2. Values of exchange interactions in $KCuCl_3$ [5] and $TlCuCl_3$ [3]. The intradimer interaction J is given in meV; interdimer interactions are given in units of J for the respective compound.

Exchange constant	$KCuCl_3$	$TlCuCl_3$
J (meV)	4.25	5.68
$J_{(100)}$	0.00	0.06
$J'_{(100)}$	0.10	0.30
$J'_{(201)}$	0.18	0.45
$J_{(1\frac{1}{2}\frac{1}{2})}$	0.20	0.16
$J'_{(1\frac{1}{2}\frac{1}{2})}$	0.05	−0.10

translational symmetry:

$$|\mathbf{q}\rangle^{(0)} = \frac{1}{\sqrt{2N}} \sum_{k=1}^{2} \sum_{\mathbf{n}} c_k \mathrm{e}^{-\mathrm{i}\mathbf{q}(\mathbf{n}+\mathbf{R}_k)} |\mathbf{n} + \mathbf{R}_k\rangle^{(0)}. \tag{14}$$

The states $|\mathbf{n}+\mathbf{R}_k\rangle^{(0)}$ denote a triplet at site $\mathbf{n}+\mathbf{R}_k$ with all the other sites occupied by singlets. We have introduced the coefficient c_k to take into account the different dimer orientations. The c_k are determined requiring that $c_1|\mathbf{n} + \mathbf{R}_1\rangle + c_2|\mathbf{n} + \mathbf{R}_2\rangle$ is diagonal in the subspace of the one-triplet excitations. Two solutions ($\pm$) are obtained:

$$(c_1^+, c_2^+) = (1, 1) \qquad \text{or} \qquad (c_1^-, c_2^-) = (1, -1). \tag{15}$$

The solution c^- is connected to umklapp scattering where $\mathbf{q} \to \mathbf{q} + \mathbf{u}$. Umklapp processes are possible in $KCuCl_3$ and $TlCuCl_3$ with an integer number of the reciprocal lattice vector $\mathbf{u} = \mathbf{b}^*$ or $\mathbf{c}^*$.

The resulting energies are denoted by $\omega^{\pm}(\mathbf{q})$, where we describe both modes in the first crystallographic Brillouin zone. Up to first order we obtain the well known dispersion relation [5, 4] in units of J:

$$\omega^{\pm}(\mathbf{q}) = 1 + 2\sum_{i=1}^{2} \beta_i \cos(\mathbf{g}_i\mathbf{q}) \pm 2\sum_{i=3}^{4} \beta_i \cos(\mathbf{g}_i\mathbf{q}) + \mathcal{O}(\lambda^2). \tag{16}$$

Here and in the following we use some shorthand for various combinations of coupling constants (ϵ_i and $\gamma_i^{\ j}$ will be needed for the intensity calculation below):

$$\begin{aligned}
&\beta_1 = \tfrac{1}{4}(2J_{(100)} - J'_{(100)}), && \varepsilon_1 = \tfrac{1}{4}(2J_{(100)} + J'_{(100)}), && \gamma_1 = \tfrac{1}{4}J'_{(100)},\\
&\beta_2 = -\tfrac{1}{4}J'_{(201)}, && \varepsilon_2 = \tfrac{1}{4}J'_{(201)}, && \gamma_2 = -\tfrac{1}{4}J'_{(201)},\\
&\beta_3 = \tfrac{1}{4}(J_{(1\frac{1}{2}\frac{1}{2})} - J'_{(1\frac{1}{2}\frac{1}{2})}), && \varepsilon_3 = \tfrac{1}{4}(J_{(1\frac{1}{2}\frac{1}{2})} + J'_{(1\frac{1}{2}\frac{1}{2})}), && \gamma_3^{\pm} = \tfrac{1}{4}(\pm J_{(1\frac{1}{2}\frac{1}{2})} + J'_{(1\frac{1}{2}\frac{1}{2})}),\\
&\beta_4 = \beta_3, && \varepsilon_4 = \varepsilon_3, && \gamma_4^{\pm} = \gamma_3^{\pm}.
\end{aligned} \tag{17}$$

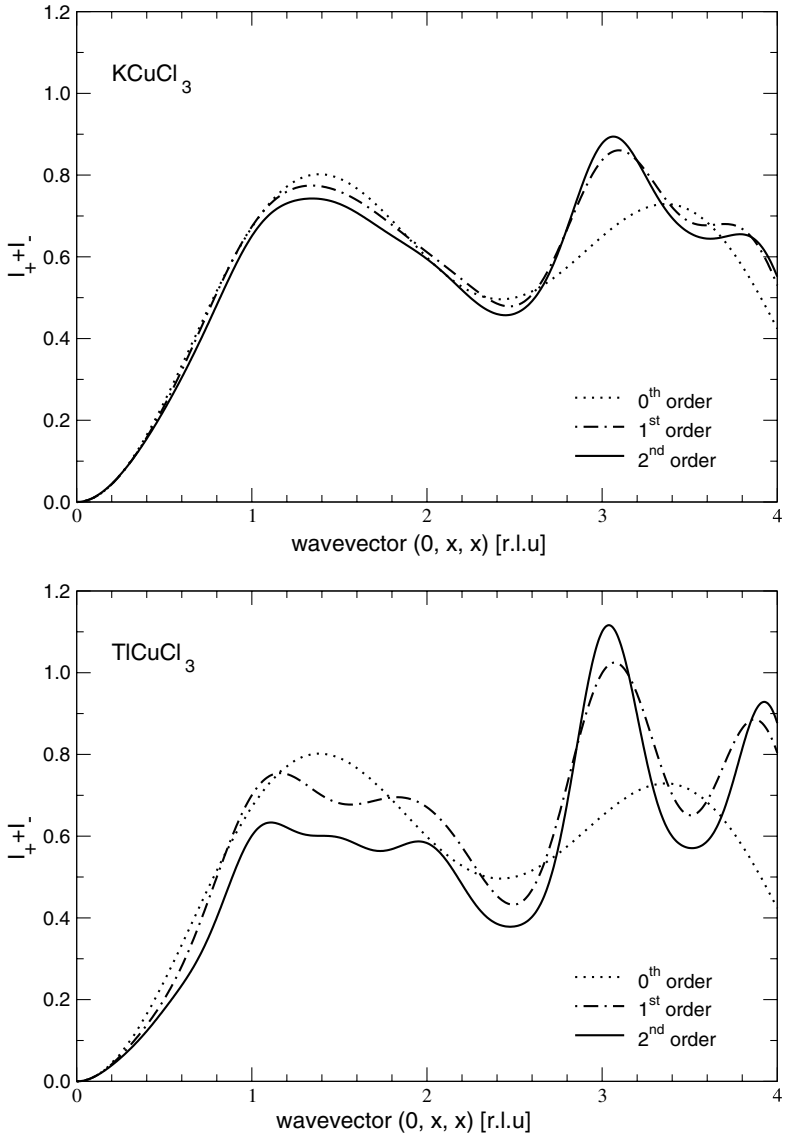

Figure 3. Total spectral weight $I_+ + I_-$ along the $(0, x, x)$ direction in zeroth, first and second order. Top panel, $KCuCl_3$; bottom panel, $TlCuCl_3$.

To obtain the transition matrix element one has to expand both the ground state and the one-triplet state perturbatively in the coupling constants. To indicate the order we take all interdimer couplings proportional to a constant λ.

3.1. The ground state

There are four different directions $\mathbf{g}_i$ in which we find interdimer interactions (see table 1). As well as in the one-dimensional case the unperturbed ground state is a product of singlets

placed on the rungs:

$$|G\rangle^{(0)} = \prod_{\mathbf{n}} |s_{\mathbf{n}+\mathbf{R}_1}\rangle |s_{\mathbf{n}+\mathbf{R}_2}\rangle = |S\rangle. \tag{18}$$

Due to the different orientations we distinguish between singlets at $\mathbf{n}+\mathbf{R}_1$ and $\mathbf{n}+\mathbf{R}_2$. Up to the second order the ground state including all relevant states for the structure factor is

$$|G\rangle^{(2)} = \alpha_0|S\rangle + \frac{\sqrt{3}}{2}\sum_{i=1}^{4}\sum_{k=1}^{2}\sum_{\mathbf{n}} \beta_i(1+\varepsilon_i)|\mathbf{n}+\mathbf{R}_k, \mathbf{n}+\mathbf{R}_k+\mathbf{g}_i\rangle^{(0,0)} \tag{19}$$

$$-\frac{\sqrt{3}}{2}\sum_{i,j=1}^{4}\sum_{k=1}^{2}\sum_{\mathbf{n}} \beta_i\beta_j|\mathbf{n}+\mathbf{R}_k, \mathbf{n}+\mathbf{R}_k+\mathbf{g}_i+\mathbf{g}_j\rangle^{(0,0)} \tag{20}$$

$$-\frac{\sqrt{3}}{2}\sum_{\substack{i,j=1\\ i\neq j}}^{4}\sum_{k=1}^{2}\sum_{\mathbf{n}} \beta_i\beta_j|\mathbf{n}+\mathbf{R}_k, \mathbf{n}+\mathbf{R}_k+\mathbf{g}_i-\mathbf{g}_j\rangle^{(0,0)} \tag{21}$$

$$+ \text{ states with three or four triplet excitations.} \tag{22}$$

The indices i, j are linked to the different interaction directions and k counts the two dimer sites in the elementary cell. We further denote the states having two triplets at sites $\mathbf{r}$ and $\mathbf{r}'$ with well defined S_{tot} and S^z_{tot} by $|\mathbf{r},\mathbf{r}'\rangle^{(S_{\mathrm{tot}},S^z_{\mathrm{tot}})}$. α_0 is a normalization factor which guarantees that $\langle G|G\rangle^{(2)} = 1+\mathcal{O}(\lambda^3)$:

$$\alpha_0 = 1 - \tfrac{3}{4}N\sum_{i=1}^{4}\beta_i^2. \tag{23}$$

Note that N labels the number of unit cells, whereas $2N$ is the number of dimers in the system.

3.2. One-triplet excitation

The expansion of the wavefunction for the one-triplet excitation in the interdimer interactions is obtained to first order by acting with the Hamiltonian $\mathcal{H}_1$ on the state (14) and some subsequent normalization. In addition to simple propagation of the triplets this leads to the generation of two-triplet excitations $|\mathbf{r},\mathbf{r}'\rangle^{(1,0)}$ where $(S_{\mathrm{tot}}, S^z_{\mathrm{tot}}) = (1,0)$ is the total spin and total magnetization and $\mathbf{r},\mathbf{r}'$ label the lattice sites occupied by triplets. There are also three-triplet excitations with the same spin quantum numbers. Second order terms contribute to the third order[4] of the intensity only and will not be calculated here. However, normalization of the wavefunction has to be done up to second order terms.

3.3. The dynamical structure factor

To leading order one expects a dimer-like structure factor as in section 2. In fact, there are two different contributions due to the two dimer structure in the elementary cell:

$$I_{\pm}(\mathbf{q}) = D^2_{\pm}(\mathbf{q}) + \mathcal{O}(\lambda^1) = \left[\sin\frac{\mathbf{q}\mathbf{d}_1}{2} \pm \sin\frac{\mathbf{q}\mathbf{d}_2}{2}\right]^2 + \mathcal{O}(\lambda^1). \tag{24}$$

The indices $\pm$ refer to (16) and correspond to symmetric (respectively antisymmetric) modes for $\mathbf{q}$ in the first Brillouin zone. However, the role of symmetric and antisymmetric modes is interchanged for $\mathbf{q} \to \mathbf{q}+\boldsymbol{\tau}$ where $\mathrm{e}^{\mathrm{i}\boldsymbol{\tau}(\mathbf{R}_2-\mathbf{R}_1)} = -1$. From now on $\mathbf{q}$ stays in the first Brillouin zone.

[4] All contributing terms can be obtained on request.

The representation of (24) is instructive in order to emphasize that in general there are contributions from two different modes for a wavevector $\mathbf{q}$ in the crystallographic Brillouin zone. The total contribution

$$I_+(\mathbf{q}) + I_-(\mathbf{q}) = 2\sin^2\frac{\mathbf{q}\mathbf{d}_1}{2} + 2\sin^2\frac{\mathbf{q}\mathbf{d}_2}{2} \tag{25}$$

reproduces correctly the structure factor $\int \mathrm{d}\omega\, S(\mathbf{q},\omega)$ as calculated from (1) in lowest order.

A finite contribution for the excitation mode with energy $\omega^-(\mathbf{q})$ requires $\mathbf{q}\mathbf{d}_1 \neq \mathbf{q}\mathbf{d}_2$. Taking into account the dimer orientations $\mathbf{d}_{1,2}$ where

$$\begin{aligned}\mathbf{d}_1 &= 0.48\mathbf{a} + 0.10\mathbf{b} + 0.32\mathbf{c},\\ \mathbf{d}_2 &= 0.48\mathbf{a} - 0.10\mathbf{b} + 0.32\mathbf{c}\end{aligned} \tag{26}$$

we deduce the condition $\mathbf{q}_b \neq 0$, in agreement with the experimental observations.

Considering higher order corrections to the ground state and the first excited state as presented below, we get the following result valid up to second order:

$$\begin{aligned}I_\pm(\mathbf{q}) = {}& \tfrac{1}{4}D_\pm^2(\mathbf{q})(1 - \Omega_\pm(\mathbf{q}) + \Omega_\pm^2(\mathbf{q}) - \Sigma_\pm(\mathbf{q}) - \Sigma_1(\mathbf{q}))\\ &+ \frac{1}{2}D_\pm(\mathbf{q})\left(\cos\frac{\mathbf{q}\mathbf{d}_1}{2} \pm \cos\frac{\mathbf{q}\mathbf{d}_2}{2}\right)\Delta_\pm(\mathbf{q})\end{aligned} \tag{27}$$

where

$$\Omega_\pm(\mathbf{q}) = 2\sum_{i=1}^{2}\beta_i\cos(\mathbf{q}\mathbf{g}_i) \pm 2\sum_{i=3}^{4}\beta_i\cos(\mathbf{q}\mathbf{g}_i), \tag{28}$$

$$\Sigma_\pm(\mathbf{q}) = \sum_{i=1}^{4}[3\beta_i^2 - \beta_i^2\cos(2\mathbf{q}\mathbf{g}_i)] + 2\sum_{i=1}^{2}\beta_i\varepsilon_i\cos(\mathbf{q}\mathbf{g}_i) \pm 2\sum_{i=3}^{4}\beta_i\varepsilon_i\cos(\mathbf{q}\mathbf{g}_i), \tag{29}$$

$$\Sigma_1(\mathbf{q}) = 4\sum_{i=1}^{2}\gamma_i^2[1 + \cos(\mathbf{q}\mathbf{g}_i)] + 2\sum_{i=3}^{4}[\gamma_i^{+2} + \gamma_i^{-2} + 2\gamma_i^+\gamma_i^-\cos(\mathbf{q}\mathbf{g}_i)], \tag{30}$$

$$\Delta_\pm(\mathbf{q}) = 2\sum_{i=1}^{2}\beta_i\gamma_i\sin(\mathbf{q}\mathbf{g}_i) + 2\sum_{i=3}^{4}\beta_i(\gamma_i^- \pm \gamma_i^+)\sin(\mathbf{q}\mathbf{g}_i). \tag{31}$$

The dynamical structure factor contains contributions from both excitation modes:

$$S^{zz}(\mathbf{q},\omega) = I_+(\mathbf{q})\delta(\omega - \omega^+(\mathbf{q})) + I_-(\mathbf{q})\delta(\omega - \omega^-(\mathbf{q})), \tag{32}$$

where $\omega^\pm(\mathbf{q})$ denotes the one-triplet excitation energy as in (16). We note that $\Omega(\mathbf{q})$ is the energy of the one-triplet excitation $\omega^+(\mathbf{q})$ up to first order. If we neglect the terms $\Sigma_i(\mathbf{q})$ and $\Delta_\pm(\mathbf{q})$ the result reduces to RPA-like calculations [9] where $I_\pm(\mathbf{q}) \propto 1/\omega^\pm(\mathbf{q})$.

In order to demonstrate the effect of interdimer interactions on the dynamical structure factor we show in figure 3 theoretical results for $KCuCl_3$ (top panel) and $TlCuCl_3$ (bottom panel) in zeroth (non-interacting dimers), first and second order; exchange parameters are taken from table 2. As in the INS experiments to be discussed in the next section and as in [9], the variation of the spectral weight of the triplet excitation $I_+ + I_-$ with wavevector is shown along the $(0, x, x)$ direction of reciprocal space, such that both modes contribute with finite weight. Evidently, higher order corrections are more important for $TlCuCl_3$ with its larger exchange constants, but even for these larger values the comparison of different orders seems to indicate convergence. Exhaustive experimental results for both I_+ and I_- are available for $KCuCl_3$ and will be discussed in the next subsection. Clearly, devoted INS experiments for $TlCuCl_3$ are of considerable interest (see also [4] and [3]); the ratio of spectral weights at wavevectors corresponding to maximum and minimum intensity appears to be a reasonable quantity to test the agreement with our theoretical results. Present results do not indicate that calculations higher than second order are required.

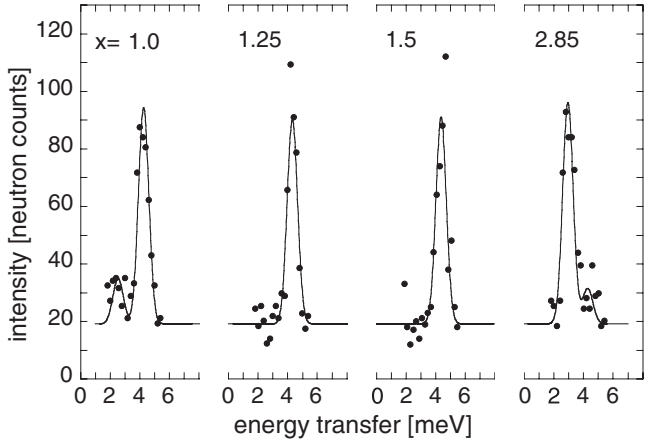

Figure 4. Typical fits of the neutron profiles for wavevectors **q** taken at selected $(0, x, x)$ values in (rlu).

3.4. Experiment

The INS results on the material $KCuCl_3$ were collected at the IN3 neutron spectrometer, Institut Laue–Langevin, Grenoble (France). Standard focusing geometry was adopted for all energy scans performed under constant final energy $E_f = 13.7$ meV. A pyrolitic graphite (PG) filter in front of the analyser was further used to suppress higher order contaminations.

The INS profiles were obtained at fixed $T = 2$ K for the wavevectors along the $(0, x, x)$ direction of reciprocal space, which is suited to demonstrate the issues introduced above. For this purpose, a $KCuCl_3$ single crystal was aligned for scattering in the b^*c^* plane. The spectral weight of the triplet excitation was determined from global least squares fits to the measured neutron profiles, assuming Gaussian peaks on top of a common background. The centre of the peaks was further fixed at the energies $\omega^{\pm}(\mathbf{q})$ resulting from the analysis presented in [5] (see table 2). Our present results complete the experimental investigation of the b^*c^* plane summarized in [4], and references therein.

In figure 4 typical fits of the neutron profiles are shown for wavevectors **q** at selected $(0, x, x)$ values, in reciprocal lattice units (rlu) of the unit cell. In accordance with the theoretical expectations, both excitation modes $\omega^{\pm}(\mathbf{q})$ are visible along $(0, x, x)$ but the spectral weight $I_{\pm}(\mathbf{q})$ strongly depends on x. Continuous curves denote the global least squares fit function, symbols the profiles in neutron counts. The statistical tolerance scales according to the neutron counts. In figure 5, the fitted spectral weight is compared to the model expectations previously introduced. In the top panel, the total spectral weight $F^2(I_+ + I_-)$ (full curve) is compared to the experimental observations (symbols). The only free parameter is an overall scaling factor accounting for the size of the sample; both the plain calculation (dashed dotted line, second order) and the squared magnetic form factor F^2 (dotted curve) [14] are shown separately for convenience. In the bottom panel, the relative spectral weight $I_+/(I_+ + I_-)(\mathbf{q})$ is compared to the experimental observations, as indicated. The graphical representation underlines the redistribution of the spectral weight among I_+ and I_- which occurs along the $(0, x, x)$ direction of reciprocal space.

From figure 5, reasonable agreement between predictions from the dimer model and experimental results is concluded. The spectral weight is dominated by the bipartite dimer structure, which governs the result in the non-interacting dimer limit, but the existence of higher

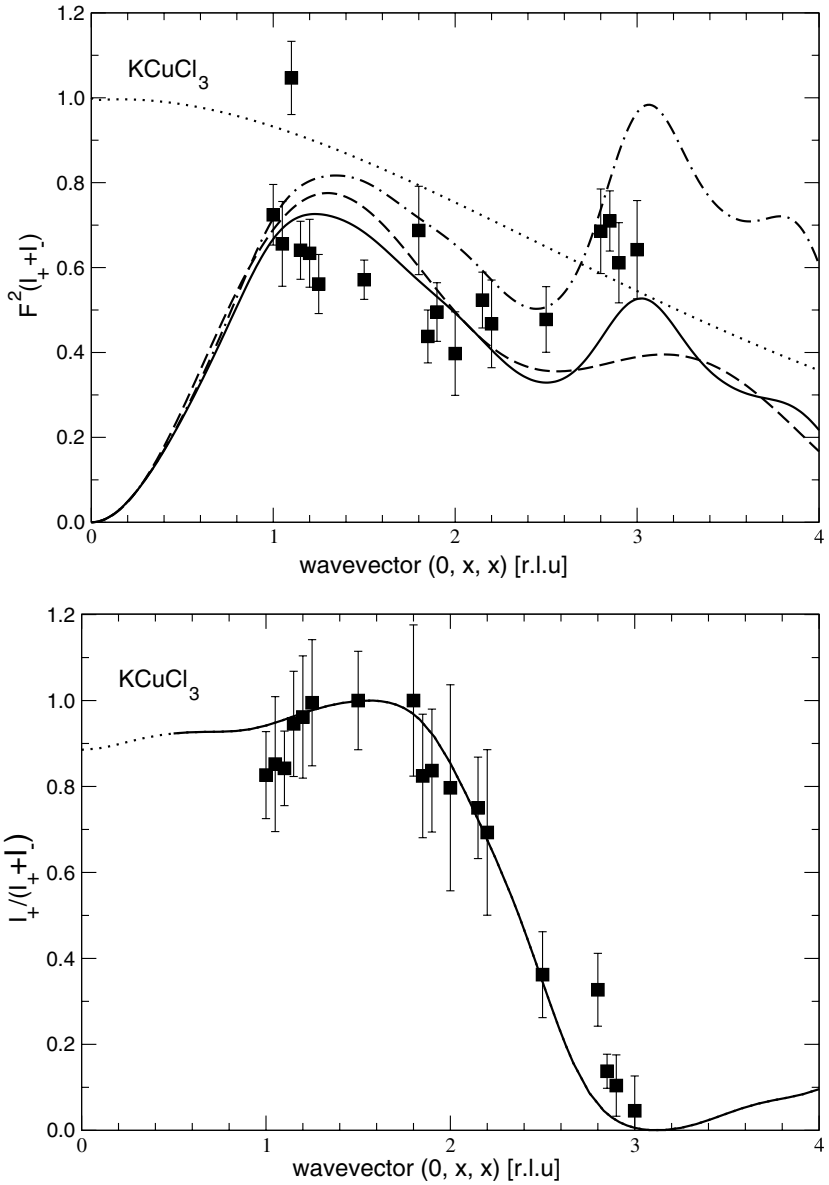

Figure 5. Spectral weight of the triplet excitation for $KCuCl_3$ along the $(0, x, x)$ direction in reciprocal space. Symbols indicate experimental data from a least squares fit to the profiles. Top panel: theoretical result for $F^2(I_+ + I_-)$ in second order (full curve) and for non-interacting dimers (dashed curve), F^2 (dotted curve) and $(I_+ + I_-)$ in second order (dash–dotted curve). Bottom panel, full curve: theoretical result in second order for the relative spectral weight.

order corrections is clearly seen close to the second maximum ($x \approx 3$). Details of higher order corrections remain almost beyond statistics for $KCuCl_3$ but may become more pronounced in the sister material $TlCuCl_3$. Our results improve on the previous RPA calculations [9] which are correct only to first order. Related investigations along different directions of the b^*c^* plane were successfully compared to RPA calculations in [15]. The relative spectral weight (bottom

panel of figure 5) is very well described already in the non-interacting dimer picture (not shown in figure 5); higher order corrections are below statistical significance for this quantity.

3.5. Sum rule

We calculate the one-magnon contribution to the total integrated scattering intensity in order to check the sum rule (12). As seen in (32) the dynamical structure factor consists of two parts. Integrating over $\mathbf{q}$, only non-oscillating terms survive, giving

$$\mathcal{I}_{\mathrm{sm}} = \tfrac{3}{4}\left[1 - \sum_{i=1}^{4} \beta_i^2 - 4(\gamma_1^2 + \gamma_2^2) - 2(\gamma_3^{+2} + \gamma_4^{+2} + \gamma_3^{-2} + \gamma_4^{-2})\right] + \mathcal{O}(\lambda^3). \tag{33}$$

Using the coupling constants as calculated in [5] we estimate here the intensity which goes into higher order scattering processes such as two- or more-magnon scattering. We obtain $\mathcal{I}_{\mathrm{sm}} = 0.7217$ which means that 96.23% of the total scattering intensity is concentrated in the lowest triplet excitation. Although the interactions in $TlCuCl_3$ are more pronounced most of the scattering intensity still goes in the one-magnon process which is reflected by inserting calculated coupling constants [3] in (33): $\mathcal{I}_{\mathrm{sm}} = 0.7021$ or 93.62% respectively. The absolute experimental determination of the spectral weight from dimers is exemplified in [16], but a devoted investigation of the materials $KCuCl_3$ and $TlCuCl_3$ has not been performed to date.

4. Conclusion

We have presented series expansions for the dynamical structure factor valid generally for lattices with two dimers per unit cell. Applying our results to the interacting dimer material $KCuCl_3$, we have shown that results obtained by inelastic neutron scattering are reasonably well described by the theoretical calculations. Our expressions apply as well to the sister material $TlCuCl_3$, which shares with $KCuCl_3$ the structure of the exchange couplings, but has larger exchange strengths. For the specific direction in $\mathbf{q}$-space considered here our results show that higher order terms are not relevant for relative spectral weights (see figure 5 as measured in $KCuCl_3$ with present intensity) and we expect that this is generally true. Second order shifts, however, show up in absolute spectral weights [17], most clearly in $TlCuCl_3$.

The materials $KCuCl_3$ and $TlCuCl_3$ have recently been demonstrated to undergo field-induced magnetic ordering. The evolution of the excitation modes at finite magnetic field has been described in a comprehensive theoretical study [18], albeit limited to the energy of the excitations. Theoretical investigations of the spectral weight in an external magnetic field are now under preparation.

Acknowledgments

The experienced support of F Demmel and A Hiess during the IN3 experiment is gratefully acknowledged. This work was partially supported by the Swiss National Science Foundation through the NCCR project MaNeP.

Appendix A. Cluster expansion

In this appendix we briefly summarize the method of cluster expansion for the dynamical structure factor in the case of the alternating chain. Some detailed considerations can be found

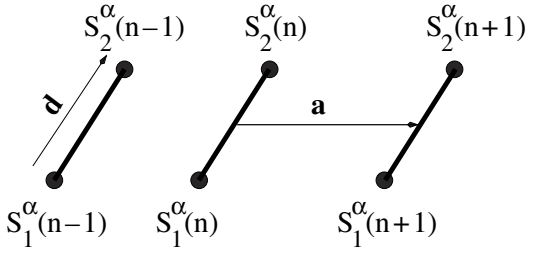

Figure A.1. Linear arrangement of dimers indicating the similarity of alternating chain (interdimer interactions only between $S_2(n)$ and $S_1(n+1)$) and ladder (general interdimer interactions) geometries.

elsewhere [19]. As shown in figure A.1, the crystallographic unit cell contains two spins. Thus the Fourier transform of the spin operator splits into two parts and reads as

$$S^\alpha(\mathbf{q}) = \sum_n \mathrm{e}^{-\mathrm{i}qna}(\mathrm{e}^{-\mathrm{i}\frac{\mathbf{qd}}{2}} S_1^\alpha(n) + \mathrm{e}^{\mathrm{i}\frac{\mathbf{qd}}{2}} S_2^\alpha(n)). \tag{A.1}$$

As before $\|\mathbf{a}\| = a$ is the distance between neighbouring spins and $\mathbf{d}$ denotes the spacing between the two spins on a dimer. In our notation q is the projection of the wavevector $\mathbf{q}$ on the chain direction.

Using translational invariance with respect to the centre of the dimer we obtain for the singlet–triplet transition amplitude

$$I_{\mathrm{sm}}(\mathbf{q}) = \sum_n \mathrm{e}^{-\mathrm{i}qan}[A_{11}^{zz}(n) + A_{22}^{zz}(n) + \mathrm{e}^{\mathbf{iqd}} A_{12}^{zz}(n) + \mathrm{e}^{-\mathbf{iqd}} A_{21}^{zz}(n)] \tag{A.2}$$

where

$$A_{ij}^{zz}(n) = \langle 0|\mathcal{S}_i^z(0)|t\rangle\langle t|\mathcal{S}_j^{z\dagger}(n)|0\rangle, \qquad i, j = 1, 2. \tag{A.3}$$

Here, the sum is taken over all integer numbers n. However, it is more convenient to calculate the functions $A_{ij}^{zz}(n)$ for positive numbers n. This is feasible making use of inversion symmetry wrt the dimer centre, implying

$$A_{11}^{zz}(-n) = A_{22}^{zz}(n) \qquad \text{and} \qquad A_{12}^{zz}(-n) = A_{21}^{zz}(n). \tag{A.4}$$

Inserting (A.4) into (A.2) one arrives at the following result:

$$I_{\mathrm{sm}}(\mathbf{q}) = 2\sum_{n>0}(A_{11}^{zz}(n) + A_{22}^{zz}(n))\cos(qna) \tag{A.5}$$

$$+ 2\sum_{n>0}(A_{12}^{zz}(n)\cos(qna - \mathbf{qd}) + A_{21}^{zz}(n)\cos(qna + \mathbf{qd})) \tag{A.6}$$

$$+ A_{11}^{zz}(0) + A_{22}^{zz}(0) + \mathrm{e}^{\mathbf{iqd}} A_{12}^{zz}(0) + \mathrm{e}^{-\mathbf{iqd}} A_{21}^{zz}(0). \tag{A.7}$$

Now, functions $A_{ij}^{zz}(n)$ enter for positive n only. In the limit of non-interacting dimers only the terms with $n = 0$ (last line) survive.

At first glance the functions $A_{ij}^{zz}(n)$ are ground-state expectation values which can be computed by the well established cluster expansion method [20]. The projection operator $\mathcal{P} = |t\rangle\langle t|$ has to be evaluated from the one-magnon states $|\psi^{(i)}\rangle$, where i labels the lattice site. By means of degenerate cluster expansion these states are generated order by order [21]. Then we find for the projection operator

$$\mathcal{P} = |1\rangle\langle 1| = \sum_{ij}(g^{-1})_{ij}|\psi^{(i)}\rangle\langle\psi^{(j)}|. \tag{A.8}$$

g is the overlapping matrix of the $|\psi^{(i)}\rangle$:

$$g_{ij} = \langle\psi^{(i)}|\psi^{(j)}\rangle. \tag{A.9}$$

To invert g we use the fact that g is the unit matrix for $\lambda \to 0$:

$$g = I + \tilde{g}. \tag{A.10}$$

Owing to the matrix norm $\|\tilde{g}\| < 1$ we apply a geometric series to invert g:

$$(I + \tilde{g})^{-1} = \sum_{i=0}^{\infty} \tilde{g}^i. \tag{A.11}$$

Now we have everything at hand to calculate the singlet–triplet intensity of the dynamical structure factor: apply degenerate perturbation theory to obtain the states $|\psi^{(j)}\rangle$ and $\mathcal{P}$. Then calculate g and invert this matrix by using (A.11). Finally, apply non-degenerate perturbation theory to compute the functions $A_{ij}^{zz}(n)$.

References

[1] Rice T 2002 *Science* **298** 760
[2] Cavadini N, Heigold G, Henggeler W, Furrer A, Güdel H-U, Krämer K and Mutka H 2001 *Phys. Rev.* B **63** 172414
[3] Oosawa A, Kato T, Tanaka H, Kakurai K, Müller M and Mikeska H-J 2002 *Phys. Rev.* B **65** 94426
[4] Cavadini N, Heigold G, Henggeler W, Furrer A, Güdel H-U, Krämer K and Mutka H 2000 *J. Phys.: Condens. Matter* **12** 5463
[5] Mikeska H-J and Müller M 2000 *J. Phys.: Condens. Matter* **12** 7633
[6] Squires G 1978 *Thermal Neutron Scattering* (Cambridge: Cambridge University Press)
[7] Cavadini N, Rüegg C, Furrer A, Güdel H-U, Krämer K, Mutka H and Vorderwisch P 2002 *Phys. Rev.* B **65** 132415
[8] Barnes T, Riera J and Tennant D A 1999 *Phys. Rev.* B **59** 11384
[9] Suzuki N, Fujimoto Y and Kokado S 2000 *Physica* B **284** 1567
[10] Brehmer S, Mikeska H and Neugebauer U 1996 *J. Phys.: Condens. Matter* **8** 7161
[11] Furrer A and Güdel H 1977 *Phys. Rev. Lett.* **39** 657
[12] Damle K and Sachdev S 1998 *Phys. Rev.* B **57** 8307
[13] Trebst S, Monien H, Hamer C J, Weihong Z and Singh R R P 2000 *Phys. Rev. Lett.* **85** 4373
[14] Brown P 1992 *International Tables for Crystallography C* (Dordrecht: Kluwer)
[15] Cavadini N, Henggeler W, Furrer A, Güdel H-U, Krämer K and Mutka H 2000 *Physica* B **276** 540
[16] Zheludev A, Shirane G, Sasago Y, Hase M and Uchinokura K 1996 *Phys. Rev.* B **53** 11642
[17] Müller M 2002 Clusterentwicklungen für dimerisierte spinsysteme *Dissertation* Hannover
[18] Matsumoto M, Normand B, Rice T and Sigrist M 2002 *Phys. Rev. Lett.* **89** 77203
[19] Gelfand M P and Singh R R P 2000 *Adv. Phys* **49** 93
[20] Gelfand M P, Singh R R P and Huse D A 1990 *J. Stat. Phys.* **59** 1093
[21] Gelfand M P 1990 *Solid State Commun.* **96** 11